ChemPubSoc Europe

DOI: 10.1002/cctc.201402861

CHEMCATCHEM Full Papers

New Catalyst Series from the Sol–Gel-Entrapment of Gold Nanoparticles in Organically Modified Silica Matrices: Proof of Performance in a Model Oxidation Reaction

Rosaria Ciriminna,[a] Alexandra Fidalgo,[b] Valerica Pandarus,[c] François Béland,[c] Laura M. Ilharco,*[b] and Mario Pagliaro*[a]

Gold nanoparticles were sol–gel-entrapped in the mesoporous structure of organically modified silica matrices, and the resulting Silia*Cat* Au materials were tested as oxidation catalysts in the model reaction of 1-phenylethanol with hydrogen peroxide. The new materials were characterized by electronic microscopy, IR spectroscopy, and cryogenic N_2 sorption. The results point to conclusions of general validity that allow us to advance towards the practical use of supported gold nanoparticles in a number of applications.

Introduction

As a result of a number of exceptional properties, which includes their biocompatible nature, plasmonic behaviour and great surface activity, Au nanoparticles are researched intensely for the development of a new generation of chemical and biological sensors,[1] therapeutic agents,[2] components in photonics and molecular electronics[3] and catalysts with a broad scope of applications.[4]

If we focus on chemical reactivity, in the mid-1980s Hutchings[5] and Haruta and co-workers[6] discovered independently that Au^{3+} and supported Au nanoparticles (NPs) are exceptionally effective redox catalytic species for acetylene hydrochlorination and CO oxidation, respectively, even at very low temperatures (up to −70 °C).

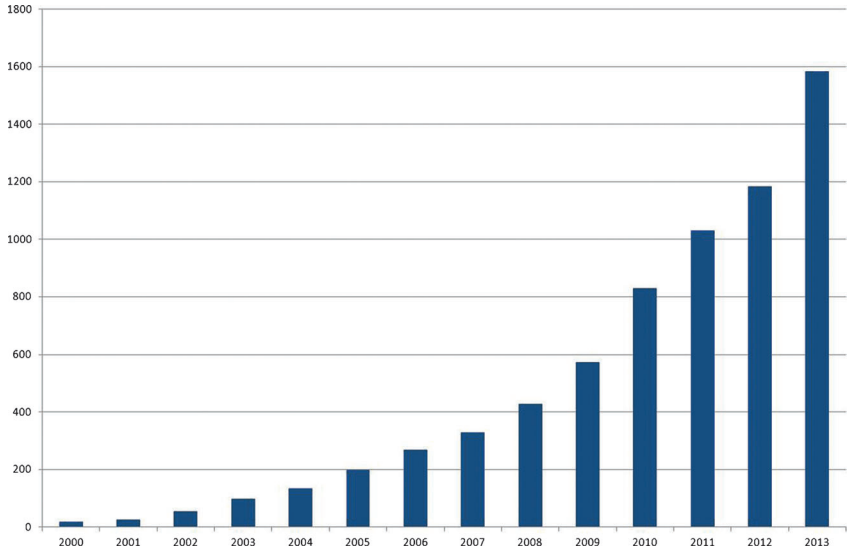

Figure 1. Trend in the number of patents that deal with Au nanochemistry (2000–2013). [Adapted from: T. Keel, Sustainable Socio-Economic Development—The Role of Gold, and Gold Mining, Electra Mining West Africa, Accra, March 2014].

Au-based catalysis has become a major topic of contemporary chemical research (Figure 1),[7] and Au-based catalysts have already been employed commercially,[8] from gas masks used in emergency situations to protect fire-fighters and miners from CO poisoning to the large-scale industrial production of vinyl acetate (in Europe and the US) over a Pd-Au catalyst supported on silica.[9]

Au NPs are oxidation catalysts of remarkable activity suitable, for example, for the direct synthesis of H_2O_2[10] and for the selective oxidation of hydrocarbons[11] with O_2 and of sugars in water.[12] In general, the catalytic activity of Au NPs is affected mainly by the particle size and the nature of the support,[13] which generally consists of activated carbons or metal

[a] *R. Ciriminna, Dr. M. Pagliaro*
Istituto per lo Studio dei Materiali Nanostrutturati, CNR
via U. La Malfa 153, 90146 Palermo (Italy)
E-mail: mario.pagliaro@cnr.it

[b] *Dr. A. Fidalgo, Prof. L. M. Ilharco*
Centro de Química-Física Molecular and IN-Institute of Nanoscience and Nanotechnology
Instituto Superior Técnico
Complexo I, Av. Rovisco Pais 1, 1049-001 Lisboa (Portugal)
E-mail: lilharco@ist.utl.pt

[c] *V. Pandarus, Dr. F. Béland*
SiliCycle Inc.
2500, Parc-Technologique Blvd, Quebec City, Quebec, G1P 4S6 (Canada)

oxides onto which Au NPs, ideally with a monomodal size distribution, are deposited.[14]

Usually, a protecting agent is used to stabilise the Au NPs at the desired small dimension to prevent agglomeration during the growth process by the creation of an organic shell that acts both as an electrostatic and steric stabiliser. For example, Hutchings and co-workers recently developed a synthetic method in which the NPs are supported over TiO_2, which starts from a solution of chloroauric acid ($HAuCl_4$) with further reduction of the Au^{3+} ions to Au^0 with a mild reductant, in the presence of polyvinyl alcohol (PVA).[15]

Tsukuda and co-workers studied the aerobic oxidation of alcohols in water mediated by polymer-stabilised Au nanoclusters and showed that the catalytic activity increases dramatically if the NPs are less than 6 nm in diameter.[16] However, the ultra-small size is not sufficient for optimal catalysis. Indeed, Hutchings and Kiely used aberration-corrected TEM to study the nature of the active site in supported Au catalysts during CO oxidation and revealed that the catalytically active species are made of bi-layers of Au NPs that involve only 7–10 Au atoms per nanoparticle.[17]

In this context of intense research on noble-metal NPs, we have lately introduced a new route to the encapsulation of metal NPs within hybrid silicas to afford a variety of sol–gel-entrapped noble-metal catalysts trade-named Silia*Cat*, which are emerging as multi-purpose mediators for numerous synthetic organic chemistry reactions.[18]

Herein, we report the synthesis and structural investigation of Au NPs sol–gel-entrapped in the aggregated mesopores of organically modified silica (ORMOSIL) matrices. The materials were employed in a representative alcohol oxidation with H_2O_2, and the results are correlated with structural aspects. TEM, N_2 adsorption, and diffuse reflectance infrared Fourier transform spectroscopy (DRIFTS) show that Au NPs are entrapped in the inner pores of the methyl silica, available for catalysis in a microenvironment that provides their chemical and physical stabilisation.

Results and Discussion

In 2009, Cao and co-workers reported the successful use of Au NPs supported on TiO_2, supplied by Mintek, as a reusable catalyst for the oxidation of various primary and secondary alcohols, which include non-activated alcohols, to the corresponding carbonyl compounds or carboxylic acids using aqueous H_2O_2 as the primary oxidant under base-free conditions.[19] Likewise, we used 1-phenylethanol as a model substrate to study the catalytic activity of the sol–gel-entrapped Au catalysts (Scheme 1).

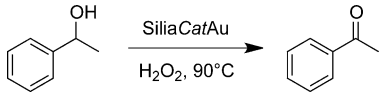

Scheme 1. Catalytic oxidation of 1-phenylethanol to acetophenone with aqueous H_2O_2 over sol–gel-encapsulated Silia*Cat* Au catalyst.

Table 1. Oxidation of 1-phenylethanol by aqueous H_2O_2 over Silia*Cat* AuRC1 and AuRC3 after 3 h.[a]

Entry	Conversion [%]	
	AuRC1	AuRC3
1st run	70	40
2nd run	64	41
3rd run	68	39

[a] Reaction conditions: 10 mmol 1-phenylethanol, 10 mL H_2O, 90 °C, 5% H_2O_2 added dropwise; substrate/H_2O_2/Au = 100:150:1. The catalyst amount used was calculated by assuming the full encapsulation of the Au precursor (chloroauric acid) in the sol–gel matrix.

The intermediate conversion (after 3 h) of 1-phenylethanol to acetophenone over 1 mol% Silia*Cat* AuRC1 and 1 mol% Silia*Cat* AuRC3 in three subsequent catalytic runs is reported in Table 1. The same catalyst was reused after it was filtered and washed.

To our delight, both AuRC1 and AuRC3 were very active catalysts. Over AuRC1, the reaction was complete after 5 h with 99% conversion to acetophenone. A slightly longer reaction time (7 h) was required for the complete reaction over AuRC3.

These results were correlated with the morphology and structure of the Silia*Cat* Au materials. The TEM images are extremely informative about the different microstructures obtained (Figure 2).

Silia*Cat* AuRC1 (5% methylated) is formed mostly by silica microparticles (100–400 nm diameter) with a considerable concentration of Au NPs (7–20 nm diameter), whereas Silia*Cat* AuRC3 (70% methylated) has less well-defined microparticles within an amorphous, sponge-like structure with a higher content of larger Au NPs (20–60 nm). It is possible that PVA was not as effective as a protective layer within the much more methylated environment of AuRC3, which allowed some agglomeration of the Au NPs before polycondensation was complete. Calcination at 250 °C, intended to remove the protective PVA, appears to have induced some further condensation and aggregation of the Au NPs.

DRIFT spectra (Figure 3 A) show the tremendous difference in methylation between AuRC3 and AuRC1, namely, in the relative intensities of the bands related to methyl groups, which are much stronger in AuRC3: $\nu_{as}(Si)CH_3$ (at $\tilde{\nu} = 2975$ and 2980 cm^{-1}, respectively, for AuRC3 and AuRC1), $\nu_s(Si)CH_3$ ($\tilde{\nu} =$ 2914 and 2919 cm^{-1}) and $\delta_s(Si)CH_3$ ($\tilde{\nu} = 1275$ and 1279 cm^{-1}). The $\rho(Si)CH_3$ mode ($\tilde{\nu} = 779$ cm^{-1} in AuRC3) is not detected in AuRC1 as it is overlapped with the ν_sSi–O–Si band at approximately $\tilde{\nu} = 800$ cm^{-1}.

The silica structure is completely different in the two samples: in the spectrum of AuRC1, the ν_{as}Si–O–Si band is broad with unresolved components and a maximum absorption at $\tilde{\nu} = 1087$ cm^{-1}, whereas in AuRC3, it is apparently split into two bands at $\tilde{\nu} = 1052$ and 1130 cm^{-1}, which are assigned to the longitudinal and transverse optical components.[20] This larger splitting between the optical components is indicative of a higher porosity.[21]

The evaluation of these structural differences from the ν_sSi–O–Si band is not straightforward because it is overlapped

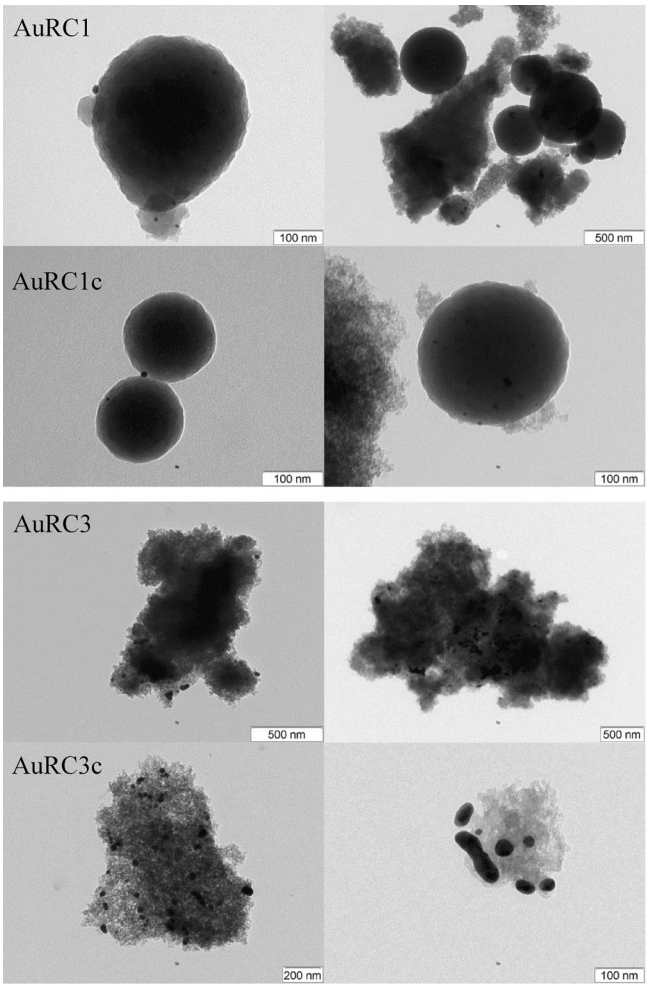

Figure 2. TEM micrographs of the Silia*Cat* Au samples.

with the ρ(Si)CH_3 mode, which is very strong in AuRC3. However, another indication of the different silica structures is given by the νSi–OH/νSi–O^- band, which appears at $\tilde{\nu}=925$ and 971 cm^{-1}, respectively, for AuRC3 and AuRC1 and is much stronger for the less methylated sample. This band usually has two components, the one at the higher wavenumber is assigned to Si–OH groups and the other to broken siloxane bridges (Si–O^-). Its different position, profile and relative intensity are consistent with a predominance of uncondensed hydroxyl groups in AuRC1.

The enhancement of the $\tilde{\nu}=2500$–4000 cm^{-1} region (Figure 3 B) allows us to complement these conclusions. The νOH band, with a maximum absorption at approximately $\tilde{\nu}=3400$ cm^{-1}, is much stronger in AuRC1, which shows a much lower degree of condensation. Moreover, the spectrum of this less methylated sample shows a νOH peak at $\tilde{\nu}=3739$ cm^{-1} assigned to free hydroxyl groups. The degree of hydrolysis is also lower for the AuRC1 sample, the spectrum of which presents a band at $\tilde{\nu}=2946$ cm^{-1}, assignable to the $\nu_{as}(O)CH_2$ mode of residual ethoxy groups. If any PVA was present before calcination, it was in such a low concentration that it does not allow identification by IR spectroscopy.

Calcination at 250 °C does not induce relevant effects on the structure of AuRC1, as the spectra obtained before and after calcination are very similar. The slight decrease in the relative intensity of the νSi–O(H) mode may account for some further condensation. However, the profile of the νOH band changes (Figure 3 B): it splits to show a minimum at $\tilde{\nu}=3420$ cm^{-1}, the relative intensity increases for higher wavenumbers at the cost of the lower wavenumber region; moreover, the intensity of the peak related to free OH groups increases. These combined observations point to a higher population of OH groups that interact less. A plausible interpretation is to assume that, although PVA was not identifiable in the spectrum of AuRC1 before calcination, some PVA molecules were hydrogen bonded to silica hydroxyl groups and removed upon calcination (PVA has a maximum νOH mode at approximately $\tilde{\nu}=3420$ cm^{-1}), which leaves a population of hydroxyl groups that interact less and a larger fraction of free ones.

In the spectra of AuRC3 before and after calcination, the differences are even more subtle: only the band at $\tilde{\nu}=925$ cm^{-1} decreases clearly, which indicates that siloxane bridges (Si–O–Si) were established upon calcination mostly between Si–O^- groups.

The N_2 adsorption–desorption isotherms of the two catalysts before calcination (Figure 4 A) show spectacular differences between them.

The adsorption isotherm of AuRC1 is clearly type IV with hysteresis type H1, characteristic of agglomerates or compacts of spheroidal particles of fairly uniform size and dispersion.[22] The specific surface area obtained by BET analysis is quite high (460 $m^2 g^{-1}$), and the total pore volume is 1.49 $cm^3 g^{-1}$ (single point at $P/P_0=0.98$). The meso-

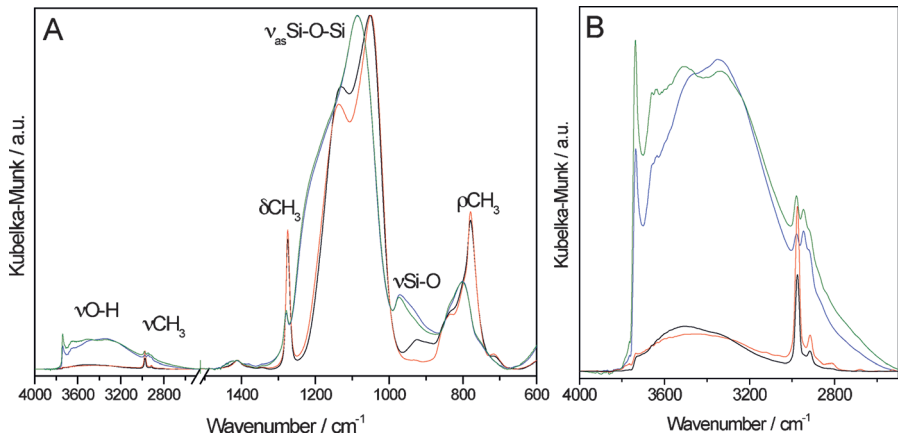

Figure 3. DRIFT spectra of Silia*Cat* Au samples normalised at the ν_{as}Si–O–Si maximum intensity: AuRC1 (——), AuRC1c (——), AuRC3 (——), AuRC3c (——). A) whole spectra and B) magnification of the high-wavenumber region.

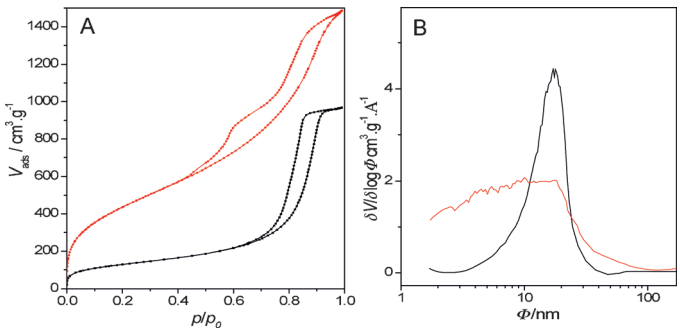

Figure 4. A) N_2 adsorption–desorption isotherms of Silia*Cat* Au samples before calcination: AuRC1 (——), AuRC3 (——). B) Corresponding BJH pore size distributions (adsorption branch).

pore size distribution, drawn from the Barrett–Joyner–Halenda (BJH) analysis of the adsorption branch (Figure 4B), shows that there is a broad range of mesopore dimensions, centred at approximately 20 nm.

For AuRC3, the adsorption isotherm is also type IV with a poorly defined high-pressure plateau, but the desorption shows two stages, indicative of a complex pore structure. Such hysteresis is consistent with a population of spheroidal particles in a mesoporous matrix, as suggested by the TEM micrographs. This kind of desorption hysteresis has been observed in flexible porous coordination polymer networks that change upon adsorption, which is responsible for a dramatic increase in the adsorption kinetics.[23]

The specific surface area and total pore volume of AuRC3 are so high ($S_{BET} = 1600\ m^2 g^{-1}$ and $V_p = 2.29\ cm^3 g^{-1}$) that this catalyst can be considered as an aerogel-like ORMOSIL with a compliant network. The BJH pore size distribution is extremely broad, with mesopores that range from 2–30 nm with a poorly defined maximum, which is consistent with a complex pore network.

For both catalysts, the large inner porosity favours the diffusion of incoming reactants to the entrapped Au NPs, whereas the large internal surface area allows the catalysts to act as molecular sponges to adsorb and concentrate the reactants in the sol–gel cages. The lower activity of the AuRC3 catalyst is ascribed to the (two times) larger size of the NPs in this material compared to that of AuRC1.

The high activity of AuRC1, which is similar to Mintek's Au/TiO_2 catalyst tested by Cao and co-workers,[19] can be explained by the fact that the methyl groups in the ORMOSIL matrix are not distributed uniformly but rather concentrate at the external surface of the cages where they enhance the cage hydrophobicity and lower the surface energy.[24]

Finally, the same $-CH_3$ groups enhance the electron density at the surface of the entrapped Au NPs, which favours the first mechanistic steps in the Au-mediated oxidation of alcohols with H_2O_2, namely, the dissociation of H_2O_2 and formation of the alcoholate (Scheme 2).[19]

These findings confirm that, as first proposed by Nørskov and co-workers who studied liquid-phase reactions mediated by heterogenised Au NPs,[25] the support (TiO_2, Fe_2O_3 and CeO_2) plays a major role in the activation of oxygen (and of H_2O_2) at the Au–support interface. If the Au NP size was the determining factor, AuRC3 (in which the NPs are as large as 60 nm) would not have a good catalytic activity under any conditions. Large differences in activity amongst distinct supported Au catalysts were also reported by Cao and co-workers in the oxidation of 1-phenylethanol with aqueous H_2O_2.[19]

Compared to Silia*Cat* Pd^0 and Silia*Cat* Pt^0, which are composed of 100% methylated matrices doped with Pd or Pt NPs, the synthetic route to Silia*Cat* Au is unique in that it requires PVA as a protecting agent, the evaporation of the reducing ethanol formed upon hydrolysis and condensation of the ethoxy silanes is not required. At a high degree of methylation, such as in the case of the 70% methylated AuRC3 catalyst, the protecting action against agglomeration of the PVA molecules is reduced and relatively large (up to 50 nm) NPs are formed.

Low alkylation of the silica matrix is known to exert a great effect in transition-metal catalysis for synthetic organic chemistry with sol–gel-entrapped catalysts,[26] which has been correlated with a significant alteration of the hydrophilic-lipophilic

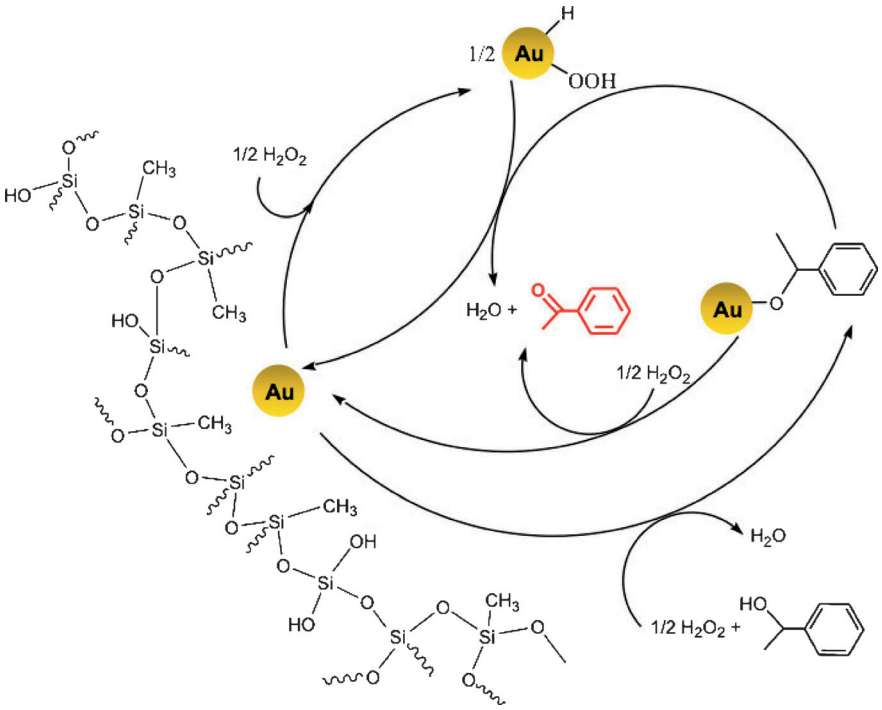

Scheme 2. Proposed mechanism of alcohol oxidation by ORMOSIL-entrapped Au catalyst using aqueous H_2O_2 as the primary oxidant. [Adapted from Ref. [19] with kind permission].

balance (HLB) of the material.[27] Here, a similar low degree of hydrophobisation ensures the formation of smaller Au particles that are well dispersed within the organosilica microparticles of high porosity. The removal of the PVA molecules by calcination further yields sol–gel cages, the surfaces of which are covered with a population of methyl groups and weakly interacting (or free) hydroxyl groups. The overall result is a material with enhanced catalytic activity coupled to excellent textural and mechanical properties, which are fundamental for practical applications.

Conclusions and Perspectives

Au nanoparticles (NPs) were sol–gel-entrapped in the mesoporous structure of methyl silica, and the resulting materials were tested in oxidation catalysis and characterised by TEM, diffuse reflectance infrared Fourier transform spectroscopy and cryogenic N_2 sorption. The results suggest the following conclusions of general validity.

First, the Au NPs are active and recyclable, despite their size in the 7–50 nm range. Second, a low (5%) degree of organic modification of the silica matrix is enough to provide a level of activity comparable to the state-of-the-art Au/TiO_2 catalyst. Third, the encapsulating matrix exercises the well-known stabilisation effects of the sol–gel cage during catalysis.[28]

Numerous research groups have studied silica-supported Au NPs. Previous studies, however, either focused on unmodified silica[29,30] or on ordered mesoporous silicas.[31] SiO_2-entrapped Au NPs are even commercially available[32] (as diagnostic agents in health applications). However, the catalytic results obtained with Au/SiO_2 are modest compared to those of Au/TiO_2 or Au/CeO_2 catalysts. For example, Au/mesoporous silica shows poor catalytic activity because a large amount of Au NPs block the mesopores and prevent reagent access to catalytically active sites, which requires entrapment of the NPs within (rather than on) the pore wall.[33]

Large-scale production of Au catalysts is difficult because of issues such as Au particle size and reproducibility. The preparation of Au catalysts also involves synthesis techniques more elaborate than the impregnation methods employed to produce Pt-group-metal catalysts. Nevertheless, it is relevant that several companies manufacture supported Au catalysts (Table 2).[34] South Africa's minerals research organisation Mintek, in particular, has been the first company to establish in 2009 a plant to manufacture significant quantities of Au-based catalysts reproducibly on different supports for use in a range of applications.

In 2000 the Au price plummeted to less than $300/oz. In October 2014, the price was $1246/oz[35] and, for comparison, the price of Pd was $775/oz[36] (heterogeneous Pd catalysts are employed widely across the chemical industry).[37] Under these circumstances, Au-based catalysis that seeks practical application will need to use ultra-low amounts of stable catalysts that are able to be recycled extensively. If these requirements are met, Au catalysis, of broad scope in the production of fine chemicals,[38] will become ubiquitous in the fine chemicals and pharmaceutical industry, as Pd catalysis is today.

To the best of our knowledge, the only application of Au NPs entrapped in organically modified silica (ORMOSIL) was reported by Ramaraj and co-workers,[39,40] who encapsulated Au/Ag bimetallic NPs in methyl-modified silica to functionalise an electrode for the electrocatalytic reduction and sensing of H_2O_2. In the present work, ORMOSIL-entrapped Au NPs have been applied successfully in catalysis by using the patented SiliaCat catalyst sol–gel process. This catalyst does not encounter any of the reproducibility difficulties encountered by deposition–precipitation methods mentioned above as it is formed entirely in the liquid phase. The loss of valued Au is prevented as generally all of the Au precursor is encapsulated smoothly in the final xerogel powder. From a green chemistry viewpoint, it is also notable that the sol–gel route for the silica-based supports takes place in an aqueous medium at room temperature and is a versatile synthetic method that allows the production of highly effective Au catalysts designed for a variety of reactions.

Table 2. Commercial Au-based catalyst applications (adapted from Ref. [34] with kind permission).

Company (Location)	Product name	Formulation	Method of manufacture	Patent	Application
Mintek (South Africa)	AUROlite	Au/TiO_2-Au/ZnO-Au/Al_2O_3	deposition precipitation	WO2005/115612	CO, VOC[a] and liquid-phase oxidation
Mintek (South Africa)	AUROlith	Au/Al_2O_3/cordierite	–	–	CO, VOC oxidation
3M (USA)	NanAuCat	Au/TiO_2/activated carbon	physical vapour deposition	WO2005/030282, WO2009/026095	CO, VOC oxidation, NASCAR[b]
Au-SDARC/Yantal University (China)	YD-2	Au-MO_x/Al_2O_3	–	WO2006/007774	CO oxidation, mine self-rescue
Novax/ITRI (Taiwan)	NGC-A+	Au/Fe_2O_3	deposition precipitation	US2004/127353	CO oxidation, fire-escape hoods
Nanostellar (USA)	NSGold	Au-Pd/Al_2O_3	deposition precipitation	WO2010/090841	diesel oxidation
TDA Research (USA)	–	Au/metal oxide	–	–	CO oxidation, military aircraft

[a] VOC = volatile organic chemical; [b] NASCAR = National association for stock car auto racing.

Experimental Section

Catalyst synthesis

Silia*Cat* Au materials were prepared by the entrapment of Au NPs in ORMOSIL matrices obtained by the sol–gel hydrolytic polycondensation of tetraethoxysilane/methyltriethoxysilane (TEOS/MTES) mixtures using different Au loads and PVA as the protecting agent. Two sets of samples were prepared: AuRC1 and AuRC3.

The typical procedure for the synthesis of Silia*Cat* AuRC1 involves three main steps. In the first one, a mixture of TEOS (95 mol%) and MTES (5 mol%) was hydrolysed by treatment with HCl (0.05 N). In the second step, a solution of $HAuCl_4$ monohydrate (0.20 g) in 3 wt% aqueous PVA was prepared and reduced with $NaBH_4$ (0.05 g). Finally, the obtained Au NPs sol was added to the pre-hydrolysed Si alkoxides mixture, and gelation was promoted through the addition of aqueous NaOH. The purple gel obtained (Figure 5) upon condensation was left to dry at RT and then powdered and used for subsequent catalytic tests.

Figure 5. A typical ORMOSIL Alcogel doped with Au NPs (AuRC1) obtained by the present sol–gel polycondensation process.

The Silia*Cat* Au RC3 sample was prepared by the same procedure starting from a mixture of TEOS (30 mol%) and MTES (70 mol%).

PVA was removed from the supported Au NPs either by heating the resulting catalysts in hot water at 90 °C under reflux (for 2 h), which did not increase the particle size and preserved the active sites associated with high catalytic activity (morphology of NPs not affected), or by calcination at 250 °C. At this temperature, the methyl groups in the organosilica matrix are preserved.[41] The synthesised samples are summarised in Table 3.

Table 3. Samples of Silia*Cat* Au.

Sample	Composition and thermal treatment
AuRC1	5%MTES+95%TEOS
AuRC1c	AuRC1 calcined at 250 °C for 3 h
AuRC3	70%MTES+30%TEOS
AuRC3c	AuRC3 calcined at 250 °C for 3 h

Material characterisation

The structural analysis of the samples was performed by DRIFTS by using a Mattson RS1 FTIR spectrometer with a Specac Selector in the 400–4000 cm^{-1} range (wide-band mercury cadmium telluride detector) at 2 cm^{-1} resolution. The spectra were the result of 1000 co-added scans for each sample in a ratio against the same number of scans for the background (ground KBr of FTIR grade Aldrich). The samples were ground and mixed with KBr in appropriate proportions to obtain spectral absorbance in the range of applicability of the Kubelka–Munk transformation.[42]

The pore structure was analysed by N_2 adsorption–desorption isothermal analysis at 77 K of the degassed samples by using a Micromeritics ASAP 2020. Degassing was performed at 200 °C for 120 min. The volume of N_2 adsorbed between two consecutive points was 15 $cm^3 g^{-1}$, and the equilibration time per point was 15 s.

The TEM micrographs were obtained by using a Hitachi H-8100 electron microscope operated at 200 kV with a LaB_6 filament. The samples were dispersed in ethanol and dropped onto a Formvar-coated Cu grid and left to evaporate.

Catalytic tests

1-Phenylethanol was used as a model substrate to study the catalytic activity of the Silia*Cat* Au materials. The oxidation of the alcohol was performed with aqueous H_2O_2 (5 wt%) as the oxidant over both AuRC1 and AuRC3 catalysts. Air was not excluded from the reaction mixture. No organic solvent was employed. In a typical catalytic run, 5% H_2O_2 (18 g) was added dropwise to a suspension of the catalyst (Au 1 mol%) in a mixture of 1-phenylethanol (1.3 g) and deionised water (10 g) in a 50 mL two-neck round-bottomed flask kept at 90 °C by using a thermostatic oil bath. After 3 h, the catalyst was removed by filtration, and the aqueous reaction mixture was extracted with ethyl acetate (EtOAc). The organic phase was analysed by GC with flame ionisation detection (FID; Shimadzu-GC 17 equipped with a Supelcowax 10 column) to determine the conversion in acetophenone. The catalyst was washed extensively (first with water and then with acetonitrile), dried at 60 °C overnight and reused as such in subsequent reaction runs under the same conditions.

Under the same reaction conditions, no alcohol oxidation was detected without added catalyst (blank test).

Acknowledgements

This article is dedicated to Professor Jochanan Blum, Hebrew University of Jerusalem, for his eminent contributions to advancing catalysis in synthetic organic chemistry. We thank Dr Trevor Keel, World Gold Council (London, UK), for kindly sharing data on the first gold-based commercial catalysts.

Keywords: alcohols · gold · nanoparticles · oxidation · sol–gel processes

[1] K. Saha, S. S. Agasti, C. Kim, X. Li, V. M. Rotello, *Chem. Rev.* **2012**, *112*, 2739 – 2779.
[2] E. C. Dreaden, M. A. Mackey, X. Huang, B. Kangy, M. A. El-Sayed, *Chem. Soc. Rev.* **2011**, *40*, 3391 – 3404.
[3] D. Conklin, S. Nanayakkara, T.-H. Park, M. F. Lagadec, J. T. Stecher, M. J. Therien, D. A. Bonnell, *Nano Lett.* **2012**, *12*, 2414 – 2419.
[4] *Modern Gold Catalyzed Synthesis* (Eds.: A. S. K. Hashmi, F. D. Toste), Wiley-VCH, Weinheim, **2012**.
[5] G. J. Hutchings, *J. Catal.* **1985**, *96*, 292 – 295.
[6] M. Haruta, T. Kobayashi, H. Sano, N. Yamada, *Chem. Lett.* **1987**, *16*, 405 – 408.
[7] G. J. Hutchings, M. Haruta, *Appl. Catal.* **2005**, *291*, 1 – 261.
[8] T. Keel, *Gold Bull.* **2013**, *46*, 1.
[9] For a thorough discussion, see: F. Gao, D. Wayne Goodman, *Chem. Soc. Rev.* **2012**, *41*, 8009 – 8020.
[10] J. K. Edwards, B. Solsona, N. B. Ntainjua, A. F. Carley, A. A. Herzing, C. J. Kiely, G. J. Hutchings, *Science* **2009**, *323*, 1037 – 1041.
[11] M. D. Hughes, Y.-J. Xu, P. Jenkins, P. McMorn, P. Landon, D. I. Enache, A. F. Carley, G. A. Attard, G. J. Hutchings, F. King, E. Hugh Stitt, P. Johnston, K. Griffin, C. J. Kiely, *Nature* **2005**, *437*, 1132 – 1135.

[12] C. Della Pina, E. Falletta, M. Rossi, *Chem. Soc. Rev.* **2012**, *41*, 350 – 369.
[13] M. Haruta, *Chem. Rec.* **2003**, *3*, 75 – 87.
[14] G. C. Bond, D. T. Thompson, *Gold Bull.* **2000**, *33*, 41 – 51.
[15] J. A. Lopez-Sanchez, N. Dimitratos, C. Hammond, G. L. Brett, L. Kesavan, S. White, P. Miedziak, R. Tiruvalam, R. L. Jenkins, A. F. Carley, D. Knight, C. J. Kiely, G. J. Hutchings, *Nat. Chem.* **2011**, *3*, 551 – 556.
[16] H. Tsunoyama, H. Sakurai, Y. Negishi, T. Tsukuda, *J. Am. Chem. Soc.* **2005**, *127*, 9374 – 9375.
[17] A. A. Herzing, C. J. Kiely, A. F. Carley, P. Landon, G. J. Hutchings, *Science* **2008**, *321*, 1331.
[18] A. Fidalgo, R. Ciriminna, L. Lopes, V. Pandarus, F. Béland, L. M. Ilharco, M. Pagliaro, *Chem. Cent. J.* **2013**, *7*, 161.
[19] J. Ni, W.-J. Yu, L. He, H. Sun, Y. Cao, H.-Y. He, K. N. Fan, *Green Chem.* **2009**, *11*, 756 – 759.
[20] A. Fidalgo, L. M. Ilharco, *Chem. Eur. J.* **2004**, *10*, 392 – 398.
[21] A. Fidalgo, M. E. Rosa, L. M. Ilharco, *Chem. Mater.* **2003**, *15*, 2186 – 2192.
[22] S. J. Gregg, K. S. W. Sing, *Adsorption, Surface Area and Porosity, 2nd ed.*, Academic Press, London, **1982**, pp. 287.
[23] D. Tanaka, A. Henke, K. Albrecht, M. Moeller, K. Nakagawa, S. Kitagawa, J. Groll, *Nat. Chem.* **2010**, *2*, 410 – 416.
[24] M. Pagliaro, R. Ciriminna, M. Wong Chi Man, S. Campestrini, *J. Phys. Chem. B* **2006**, *110*, 1976 – 1988.
[25] T. V. W. Janssens, B. S. Clausen, B. Hvolbæk, H. Falsig, C. H. Christensen, T. Bligaard, J. K. Nørskov, *Top. Catal.* **2007**, *44*, 15 – 26.
[26] R. Abu-Reziq, D. Avnir, J. Blum, *Angew. Chem. Int. Ed.* **2002**, *41*, 4132 – 4134; *Angew. Chem.* **2002**, *114*, 4306 – 4308.
[27] R. Ciriminna, L. M. Ilharco, A. Fidalgo, S. Campestrini, M. Pagliaro, *Soft Matter* **2005**, *1*, 231 – 237.
[28] R. Ciriminna, P. Demma Carà, M. Sciortino, M. Pagliaro, *Adv. Synth. Catal.* **2011**, *353*, 677 – 687.
[29] Y. Kobayashi, M. A. Correa-Duarte, L. M. Liz-Marzán, *Langmuir* **2001**, *17*, 6375 – 6379.
[30] N. M. Bahadur, S. Watanabe, T. Furusawa, M. Sato, F. Kurayama, I. A. Siddiquey, Y. Kobayashi, N. Suzuki, *Colloids Surf. A* **2011**, *392*, 137 – 144.
[31] N. Masoud, T. Duurkoop, A. van de Glind, K. P. de Jong, P. E. de Jongh, Gold catalysts stabilized inside mesoporous silica structures with different cage and entrance size, *PREPA 11—The 11th International Symposium on the Scientific Bases for the Preparation of Heterogeneous Catalysts*, Louvain-la-Neuve, 1 – 6 July 2014.
[32] For example, at nanoComposix, see: http://nanocomposix.eu/collections/silica-coated-gold (last accessed: October 22, 2014).
[33] X. Wang, L. Chen, M. Shang, F. Lin, J. Hu, R. M. Richards, *Nanotechnology*, **2012**, *23*, 294101.
[34] Applications and Future Trends in Gold Catalysis T. Keel, J. McPherson in *Environmental Catalysis Over Gold-Based Materials* (Eds.: G. Avgouropoulos, T. Tabakova), RSC Publishing, Cambridge, **2013**, Chap. 7.
[35] See charts at: www.nasdaq.com/markets/gold.aspx (last accessed: October 22, 2014).
[36] See charts at: www.nasdaq.com/markets/palladium.aspx (last accessed: October 22, 2014).
[37] See the forthcoming (2015) Pd-catalysis-themed issue of *ChemCatChem* edited by M. Pagliaro and P. Fornasiero.
[38] T. Mallat, A. Baiker, *Annu. Rev. Chem. Biomol. Eng.* **2012**, *3*, 11 – 28.
[39] G. Maduraiveeran, R. Ramaraj, *J. Electroanal. Chem.* **2007**, *608*, 52 – 58.
[40] S. Manivannan, R. Ramaraj, *J. Chem. Sci.* **2009**, *121*, 735 – 743.
[41] Z. Zhang, Y. Tanigami, R. Terai, H. Wakabayashi, *J. Non-Cryst. Solids* **1995**, *189*, 212 – 217.
[42] P. Kubelka, F. Z. Munk, *Tech. Phys.* **1931**, *12*, 593 – 601.

Received: October 25, 2014
Published online on December 10, 2014